$E1$-$M1$ Damping Interference in the Electric Field Quenching of Metastable Ar^{17+} Ions

R. W. Dunford, D. S. Gemmell, M. Jung, and E. P. Kanter
Physics Division, Argonne National Laboratory, Argonne, Illinois 60439

H. G. Berry and A. E. Livingston
Department of Physics, University of Notre Dame, Notre Dame, Indiana 46556

S. Cheng and L. J. Curtis
Department of Physics and Astronomy, University of Toledo, Toledo, Ohio 43606
(Received 7 July 1997)

We have confirmed the prediction of a pseudo-time-reversal-odd anisotropy proportional to $\vec{E} \cdot \hat{k}$ in the decay of metastable $(2s_{1/2})$ Ar^{17+} ions in an electric field $\vec{E}$, where $\hat{k}$ is the direction of observation. The anisotropy arises from interference between the $M1$ and induced $E1$ amplitudes for the decay. Theory predicts that the pseudo-T-odd invariant should contribute to the angular distribution through a term associated with the damping (finite lifetime) of the $2p$ levels. The decay rate for the interference term is found to be $-1.64(0.12)\ s^{-1}\,sr^{-1}\ (V/cm)^{-1}$. This corresponds to a $2s$ Lamb shift for Ar^{17+} of 38.6(1.4) THz. [S0031-9007(97)04308-1]

PACS numbers: 32.60.+i, 12.20.Fv, 32.30.Rj, 32.70.Cs

When two or more different multipoles contribute significantly to the decay of a quantum system, interferences among the different transition amplitudes lead to polarization and/or anisotropy of the decay radiation. Measurements of these effects can provide information on the structure or symmetries of the system [1]. In atomic physics, the anisotropy in the decay of an unpolarized metastable H-like atom in a static electric field $\vec{E}$ has been exploited to make precision atomic structure measurements [2–4]. Assuming polarization-insensitive photon detectors, only two terms contribute to the anisotropy. The first is proportional to the rotational invariant $(\vec{E} \cdot \hat{k})^2$, where $\hat{k}$ is the direction of observation of the photon. This term is part of the $E1$ decay rate caused by the Stark mixing of the $2s_{1/2}$ and $2p$ levels by the electric field and leads to a difference in the intensity of the radiation perpendicular and parallel to the electric field. It has been used to measure the Lamb shift in hydrogenic ions [5–7]. The other term is proportional to the invariant $\vec{E} \cdot \hat{k}$ and arises from interference between the $M1$ and the Stark-induced $E1$ amplitudes for the decay. It is of particular interest because it is an example of a pseudo-time-reversal (T) odd angular distribution arising from a theory which is invariant under time reversal. Other examples include effects caused by final-state interactions in nuclear beta decay [8], and pseudo-T-odd anisotropies which have been observed in the electric field quenching of polarized atoms [9,10]. With respect to the invariant $\vec{E} \cdot \hat{k}$, simply reversing $\hat{k}$ does not produce the time reversed state of the system. The true time reversed state involves an electromagnetic wave converging on the ion.

The $\vec{E} \cdot \hat{k}$ anisotropy was first discussed by Mohr [11] who showed theoretically that it gives a nonzero contribution to the angular distribution from quenching of an H-like $2s_{1/2}$ state and is associated with the damping (widths) of the $2p_{1/2}$ and $2p_{3/2}$ levels. We call it the $E1$-$M1$ damping interference term. In this Letter we report the first measurement of this effect. Our results provide confirmation of the theory of damped states in atomic physics and illustrate that a pseudo-T-odd angular distribution can occur in a T-even theory. The experiment also demonstrates a new method for determination of the Lamb shift in hydrogenic ions.

The detailed theory of the angular distribution and polarization of the radiation from Stark quenching of H-like atoms has been derived by Hillery and Mohr [4] and by van Wijngaarden and Drake [2]. The single-photon differential decay probability for unpolarized metastable ions, if the detectors are insensitive to photon polarization, has the form

$$\frac{dR_{1\gamma}}{d\Omega} = a_{M1} + a_0 E^2 + a_1 \vec{E} \cdot \hat{k} + a_2[\tfrac{3}{2}(\hat{E} \cdot \hat{k})^2 - \tfrac{1}{2}]. \quad (1)$$

In the notation of Hillery and Mohr [4] the coefficient of the $\vec{E} \cdot \hat{k}$ term is given by

$$a_1 = \frac{\alpha k_1}{\pi}[2\,\mathrm{Im}(\eta) I_{M1} J_{E1} R_{ps}^{(1/2)} + \sqrt{2}\,\mathrm{Im}(\rho) I_{M1}(K_{E1} - \sqrt{3}\,K_{M2}) R_{qs}^{(1/2)}], \quad (2)$$

where I_{M1}, J_{E1}, K_{E1}, and K_{M2} are functions associated with magnetic dipole ($M1$), electric dipole ($E1$), and magnetic quadrupole ($M2$) radiation. The subscripts p and q refer to the $2p_{1/2}$ and $2p_{3/2}$ levels, respectively, and k_1 is the $1s_{1/2}$-$2s_{1/2}$ energy difference. The Stark mixing

involves matrix elements $R_{ps}^{(1/2)}$ and $R_{qs}^{(1/2)}$ and energy denominators

$$\eta = (S + \tfrac{1}{2} i\Gamma_p)^{-1} \tag{3}$$

and

$$\rho = (\Delta E - S - \tfrac{1}{2} i\Gamma_q)^{-1}, \tag{4}$$

where S is the Lamb shift, ΔE is the fine structure splitting, and $\Gamma_{p,q}$ are the levels widths. Note that the coefficient a_1 depends on the imaginary parts of the parameters η and ρ and vanishes if the level widths are set to zero.

In the experiment, a 379-MeV beam of argon ions was supplied by Argonne National Laboratory's heavy-ion linear accelerator, ATLAS. The ions were stripped in a 200 $\mu g/cm^2$ carbon foil at the exit of ATLAS and the 18+ charge state was magnetically selected and directed to our target chamber (see Fig. 1). The Ar^{18+} ions traversed a thin (5–10 $\mu g/cm^2$) carbon foil at the chamber entrance. The emerging beam contained ions in the metastable $2s_{1/2}$ level in H-like Ar. These proceeded to the observation region where their decay radiation was monitored by two Si(Li) x-ray detectors located on opposite sides of the beam. The detectors were collimated so that they viewed a 1.9 cm region along the beam. A magnetic field $\vec{B}$ was applied perpendicular to both the beam velocity and the detector axis using permanent magnets. Because of their velocity $\vec{\nu}$ in this field, the ions experienced an electric field $\vec{E} = \gamma \frac{\vec{\nu}}{c} \times \vec{B}$ in their rest frames where $\gamma = 1/\sqrt{1 - (\nu/c)^2}$. The electric field was parallel to the axis of the detectors. Five sets of matched pairs of permanent magnets were used to provide fields ranging from 1.5 to 4.5 kG (corresponding to electric fields of 6.3×10^4 V/cm to 1.9×10^5 V/cm). Precision alignment slots in the chamber lids allowed the field to be changed and reversed precisely and reproducibly. The field produced by each set of magnets was mapped before and after the run, and the reproducibility of the field maps following a change or reversal of the magnets was checked.

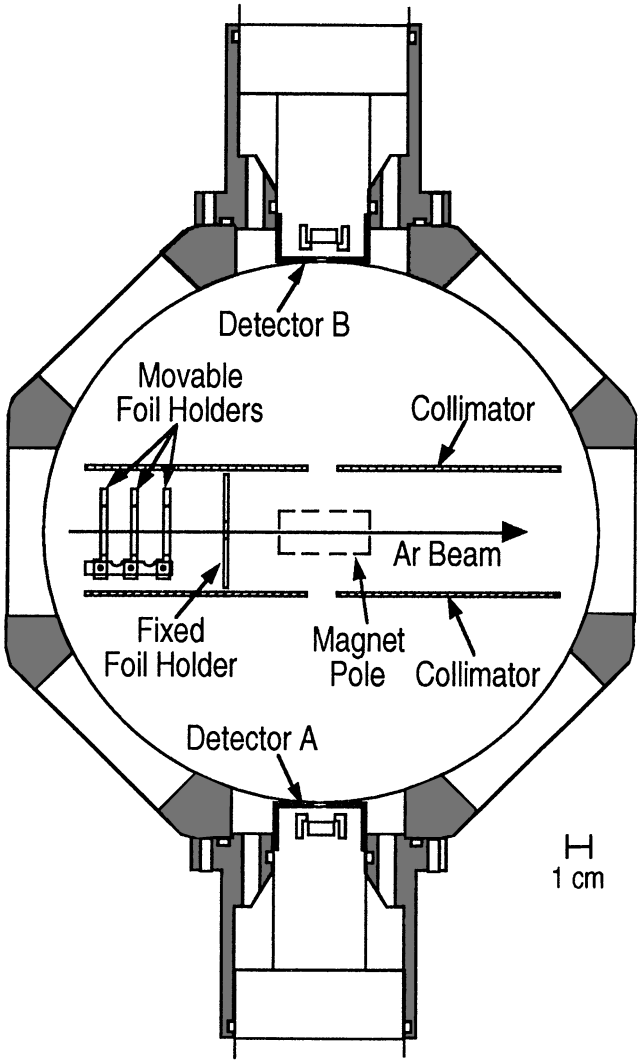

FIG. 1. Target chamber viewed from above.

In Fig. 2 we show typical spectra taken with one of the Si(Li) detectors at several values of magnetic field. The continuum radiation at energies less than 3 keV is largely due to the two-photon decay of the $2s_{1/2}$ level. The asymmetric peak near 3 keV in the field-free curve ($B = 0$) is a blend of three contributions: (i) $M1$ decays of the $2s_{1/2}$ level in H-like Ar, (ii) cascade fed decays of the $2p_{1/2}$ and $2p_{3/2}$ levels in H-like Ar, and (iii) $K\alpha$ radiation from He-like Ar. The transition energy for the latter contribution is 190 eV lower than that of the first two (Lyman-α), and this is comparable to our detector

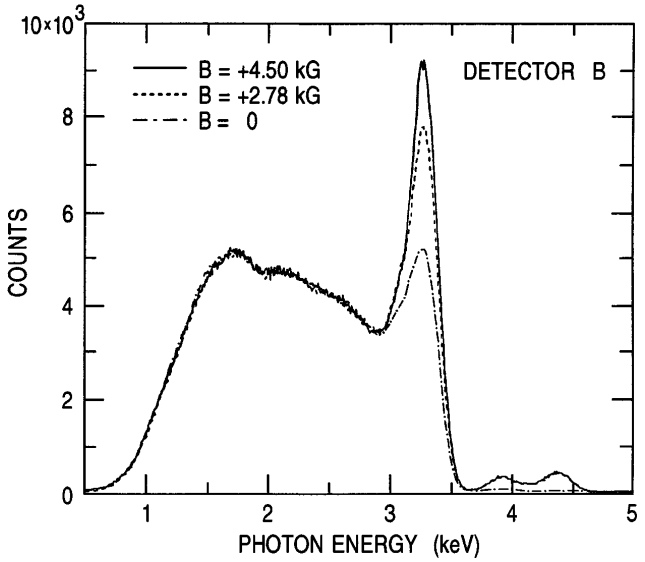

FIG. 2. Spectrum measured in detector B for three different values of the magnetic field for Ar^{18+} on a 5 $\mu g/cm^2$ foil located 9 cm from the center of the chamber. Solid curve corresponds to a 77 min integration time at a beam current of 21 nA. Other curves were normalized to give the same counts in the region 2.2–2.9 keV. The peaks near 4 and 4.5 keV appear when the field is on. They are ground state transitions from $n = 3$ and higher levels out to the Lyman series limit.

resolution. The H-like and He-like components can be reliably separated in the data analysis using a Gaussian-peak-fitting program. It is not possible to separate the contributions to the Lyman-α radiation from the $2p_{1/2}$, $2p_{3/2}$, and $2s_{1/2}$ levels in our experiment.

When a magnetic field was applied to the beam, the intensity of the Lyman-α line increased (Fig. 2), mostly due to the quenching of the metastable ions. However, the intensity as a function of the field strength does not follow the dependence expected from Eq. (1), because the field also perturbs the higher excited states that feed the cascade contribution. Figure 3 illustrates the effect of reversing the 4.5 kG magnetic field. The change in the intensity of the Lyman-α peak arises from the change in sign of the $\vec{E} \cdot \hat{k}$ interference term.

For a given run, the difference in Lyman-α counts in the two detectors can be related to the $E1$-$M1$ damping asymmetry using Eq. (1) with the result

$$N_{1\gamma}^{A} - N_{1\gamma}^{B} = 2a_1 \vec{E} \cdot \hat{k} \varepsilon_{\text{Ly-}\alpha} I_{2s} T \,, \tag{5}$$

where $N_{1\gamma}^{A}$ and $N_{1\gamma}^{B}$ are the number of counts in the H-like peak of detectors A and B (determined by the Gaussian-peak-fitting program), T is the counting time, I_{2s} is the intensity of the $2s_{1/2}$ ions, and $\varepsilon_{\text{Ly-}\alpha}$ is the overall efficiency for recording a Lyman-α photon emitted anywhere along the beam (approximately the same for each detector). We normalized the data by dividing by the counts in a region of the continuum to the low energy side of the Kα peak which arise mainly from the two-photon decay of the $2s_{1/2}$ level.

The data consist of 58 runs of 1–2 hours integration time each. For each run we formed the ratio

$$r_1 = \frac{N_{1\gamma}^{A} - N_{1\gamma}^{B}}{N_{2\gamma}^{A} + N_{2\gamma}^{B}} \,, \tag{6}$$

where the $N_{2\gamma}^{A}$ and $N_{2\gamma}^{B}$ were obtained by integrating the continuum from 2.3 to 2.6 keV for detectors A and B then subtracting a small number of counts to correct for: (i) the He-like two-photon decays, (ii) the tails from the H-like and He-like single photon peaks, and (iii) a flat background determined from a high energy (5–9 keV) region of each spectrum.

For each set of runs corresponding to a given foil, magnet, and target position, we found the average values of the ratios $\langle r_1^{+} \rangle$ and $\langle r_1^{-} \rangle$ where the superscript $\pm$ refers to the direction of the magnetic field. We then formed the quantity r_2 defined as

$$r_2 = \frac{1}{2}(\langle r_1^{+} \rangle - \langle r_1^{-} \rangle) \,. \tag{7}$$

In Fig. 4 we show r_2 plotted as a function of magnetic field for 17 runs which used the same foil and foil position. The errors in each point include the statistical uncertainty and systematic errors from misalignment, backgrounds, and differences in detector efficiency, all added in quadrature.

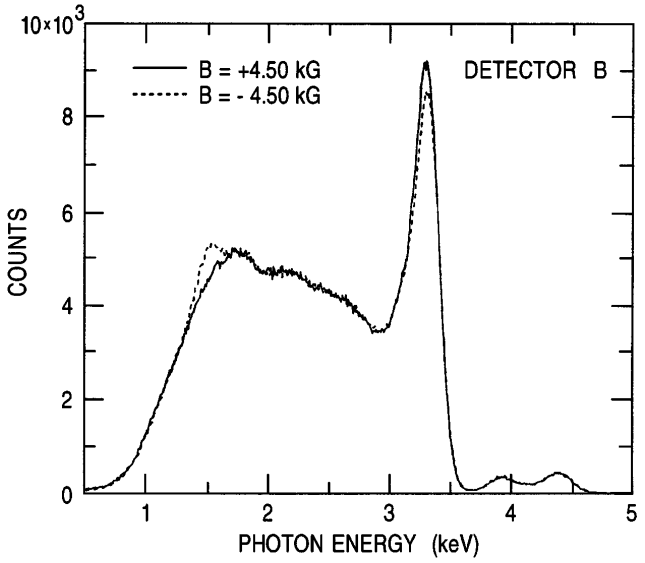

FIG. 3. Detector B spectrum for two signs of the magnetic field. The asymmetry in aluminum x-rays at 1.5 keV is caused by beam deflection. This effect is understood and does not affect our result.

These data were fit to a straight line going through the origin with the result

$$r_2 = (-0.01\,666 \pm 0.000\,41) B(\text{kG}) \,. \tag{8}$$

Converting B to the corresponding motional electric field and correcting for the detector efficiency using a Monte Carlo simulation of the experiment [12], we arrived at an experimental determination of the ratio of the coefficient a_1 of the $\vec{E} \cdot \hat{k}$ invariant [4] to the two-photon differential decay rate,

$$\left(\frac{a_1}{\omega_{2E1}/4\pi} \right)_{\text{exp}} = -7.45(0.54) \times 10^{-8} \ (\text{V/cm})^{-1} . \tag{9}$$

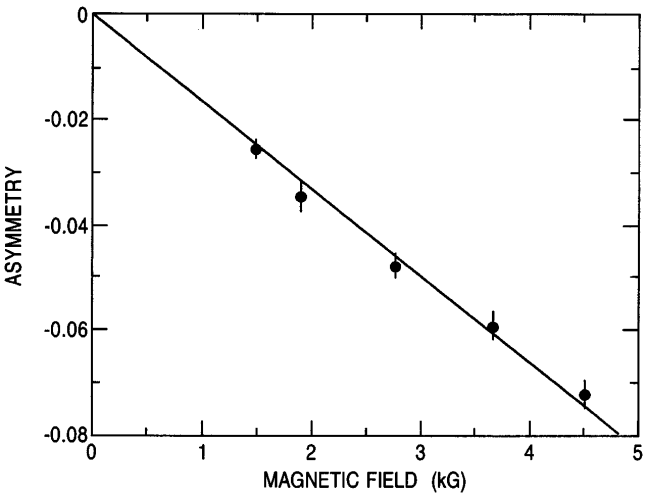

FIG. 4. $E1$-$M1$ damping asymmetry r_2 (see text) vs magnetic field strength. Each point is an average over several individual runs. For 5 μg/cm^2 foil located 9 cm from the center of the target chamber.

TABLE I. Typical corrections and uncertainties.

	4.5 kG		1.51 kG
Individual field result[a] (r_2)	-0.0725 ± 0.0032		-0.0256 ± 0.0018
Beam movement	-0.0011 ± 0.0002		$(-4.4 \pm 2) \times 10^{-4}$
Background/cascade asymmetry	0 ± 0.0025		0 ± 0.001
Peak fitting function	0 ± 0.001		0 ± 0.001
Misalignment (1st order)	0 ± 0.0016		0 ± 0.0005
Misalignment (2nd order)	$(-3 \pm 3) \times 10^{-4}$		$(-1 \pm 1) \times 10^{-4}$
Zeeman effect	$<10^{-5}$		$<10^{-7}$
Fit to r_2 vs B		(-0.0166 ± 0.00041) kG^{-1}	
Linear fitting function error[b] (%)		± 6.0	
Magnetic field (%)		± 0.5	
Beam velocity (%)		± 0.5	
Monte Carlo error (%)		± 3.0	
Final result (a_1)		(-1.64 ± 0.12) s^{-1} sr^{-1} (V/cm)$^{-1}$	

[a]Includes statistical uncertainty and corrections such as dilution of asymmetry due to finite solid angle.
[b]From comparison of the slopes obtained using one- and two-parameter fits.

Multiplying this by the theoretical value for the $2E1$ decay rate [13,14], we obtained a value for the coefficient a_1,

$$(a_1)_{\rm exp} = -1.64(0.12)\ {\rm s}^{-}\ {\rm sr}^{-1}\ ({\rm V/cm})^{-1}. \qquad (10)$$

Table I gives the final result and the typical corrections and uncertainties associated with detection efficiencies, misalignment angles, beam movement, and fitting the data.

The experimental value for the coefficient a_1 [Eq. (10)] agrees well with the theoretical value [4],

$$(a_1)_{\rm th} = -1.672\,82\ {\rm s}^{-1}\,{\rm sr}^{-1}\ ({\rm V/cm})^{-1}. \qquad (11)$$

We can also interpret the present experiment as a test of QED by setting Eq. (10) equal to Eq. (2) and solving for the Lamb shift, setting all other parameters equal to their theoretical values [4,14,15]. This gives

$$S_{\rm exp} = 38.6(1.4)\ {\rm THz}, \qquad (12)$$

in agreement with the theoretical result [16] of $S_{\rm th} = 38.19(6)$ THz, and the more precise experimental result of Gould and Marrus [17] $S_{\rm GM} = 37.89(0.38)$ THz.

Thus, our results confirm the theoretical prediction that the pseudo T-odd invariant $\vec{E} \cdot \hat{k}$ contributes to the angular distribution for the decay of an unpolarized metastable H-like ion in the presence of an electric field. They also demonstrate a new method for determining the Lamb shift in a hydrogenic atom which could have application for testing QED in ions with nuclear charges in the regime of $Z = 10$ to 25, where the $M1$ decay rate is not too small and where it is possible to observe Stark quenching with practical laboratory fields.

We are indebted to the staff of ATLAS for excellent technical assistance during this experiment. We particularly thank B. J. Zabransky and C. Kurtz for the design of the interaction region and R. Pardo and E. Rehm for assistance with the magnetic field. This work was supported by the U.S. DOE, Office of Basic Energy Sciences, Division of Chemical Sciences under Contracts No. W-31-109-ENG-38 (ANL), No. DE-FG02-92ER14-283 (University of Notre Dame), and No. DE-FG02-94ER14461 (University of Toledo).

[1] J. J. Sakurai, *Invariance Principles and Elementary Particles* (Princeton University Press, Princeton, NJ, 1964).
[2] A. van Wijngaarden and G. W. F. Drake, Phys. Rev. A **25**, 400 (1982).
[3] R. W. Dunford and R. R. Lewis, Phys. Rev. A **23**, 10 (1981).
[4] M. Hillery and P. J. Mohr, Phys. Rev. A **21**, 24 (1980).
[5] B. Curnutte, C. L. Cocke, and R. D. Dubois, Nucl. Instrum. Methods Phys. Res. **202**, 119 (1982).
[6] A. van Wijngaarden and G. W. F. Drake, Phys. Rev. A **17**, 1366 (1978).
[7] G. W. F. Drake, J. Patel, and A. van Wijngaarden, Phys. Rev. Lett. **60**, 1002 (1988).
[8] C. G. Callan and S. B. Treiman, Phys. Rev. **162**, 1494 (1967).
[9] L. P. Lévy and W. L. Williams, Phys. Rev. Lett. **48**, 1011 (1982).
[10] G. W. F. Drake, J. Patel, and A. van Wijngaarden, Phys. Rev. A **28**, 3340 (1983).
[11] P. J. Mohr, Phys. Rev. Lett. **40**, 854 (1978).
[12] R. Ali, I. Ahmad, R. W. Dunford, D. S. Gemmell, M. Jung, E. P. Kanter, P. H. Mokler, H. G. Berry, A. E. Livingston, S. Cheng, and L. J. Curtis, Phys. Rev. A **55**, 994 (1997).
[13] S. P. Goldman and G. W. F. Drake, Phys. Rev. A **24**, 183 (1981).
[14] F. A. Parpia and W. R. Johnson, Phys. Rev. A **26**, 1142 (1982).
[15] W. R. Johnson and G. Soff, At. Data Nucl. Data Tables **33**, 405 (1985).
[16] P. J. Mohr, in *Atomic Molecular, and Optical Physics Handbook*, edited by G. W. F. Drake (AIP, Woodbury, New York, 1996), p. 341.
[17] H. Gould and R. Marrus, Phys. Rev. A **28**, 2001 (1983).